Journal of Inflammation Research

Dovepress
open access to scientific and medical research

Open Access Full Text Article

ORIGINAL RESEARCH

The Combination of Gastrodin and Gallic Acid Synergistically Attenuates AngII-Induced Apoptosis and Inflammation via Regulation of Sphingolipid Metabolism

Shangtao Wang[1], Chenghao Zhu[1], Shurui Zhang[1], Siyu Ma[1], Baoshan Li[1], Shengbo Zhao[2], Wei Zhang[3], Zhirong Sun[1]

[1]School of Chinese Materia Medica, Beijing University of Chinese Medicine, Beijing, People's Republic of China; [2]Ningqiang Tianma Research Institution Limited Liability Company, Hanzhong, Shaanxi, People's Republic of China; [3]Ningqiang County Traditional Chinese Medicinal Industry Development Center, Hanzhong, Shaanxi, People's Republic of China

Correspondence: Zhirong Sun, School of Chinese Materia Medica, Beijing University of Chinese Medicine, Northeast Corner of the Intersection of Yangguang South Street and Baiyang East Road, Fangshan District, Beijing, 102401, People's Republic of China, Email szrbucm67@163.com

Video abstract

Point your SmartPhone at the code above. If you have a QR code reader the video abstract will appear. Or use: https://youtu.be/3gfkV4evN70

Background: Hypertension (HTN) is closely related to endothelial damage. While tianma (TM) and gouqizi (GQZ) have the potential to be effective in the treatment of HTN in traditional Chinese medicine, their main active ingredients and whether its exert synergistic effects and the underlying mechanisms of synergistic effects are still unclear.

Objective: This study screened the active ingredients of TM and GQZ, investigated the synergistic effects of the active ingredients and explored possible mechanisms.

Methods: The potential targets and mechanisms of TM and GQZ were screened using network pharmacology, and gastrodin (GAS) and gallic acid (GA) were identified as compounds with significant antihypertensive activity. The synergistic effects of the combination of GAS and GA was assessed by measuring biomarkers of AngII-induced human umbilical vein endothelial cell (HUVECs) dysfunction model. Furthermore, the anti-apoptotic and anti-inflammatory effects were evaluated by measuring inflammatory cytokine secretion, and apoptosis-related markers. Finally, key targets of the sphingolipid signaling pathway were experimentally validated by Western blotting.

Results: In network pharmacology, the herb-pair exerted a synergetic effect by regulating sphingolipid pathways. The GAS and GA exerted synergistic protective effects in AngII-induced HUVECs injury by improving Nitric Oxide Content (NO) levels, alleviating lactate Endothelin-1 (ET-1), and Thromboxane B2 (TX-B2) release, reducing the secretion of inflammatory factors like interleukin-6 (IL-6), interleukin-1β (IL-1β), Tumor Necrosis Factor Alpha (TNF-α)), decreasing the pro-apoptotic protein BAX, and increasing the anti-apoptotic protein BCL-2. Furthermore, the results showed that the GAS and GA combination could elevate the level of S1PR1 and inhibit the expression of ROCK2 and the phosphorylation of NF-κB, which are key targets involved in sphingolipid pathways.

Conclusion: Our study revealed that the combination of GAS and GA could suppress inflammation and apoptosis, which are highly correlated with sphingolipid signaling pathways, making it a potential candidate for the treatment of HTN.

Keywords: gastrodin, gallic acid, synergistic effects, inflammation, apoptosis, sphingolipid pathways

Introduction

Hypertension (HTN) is a chronic condition characterized by sustained elevation in systemic arterial blood pressure and is the predominant cause of mortality and morbidity global scale.[1–3] The pathogenesis of HTN is complex, and includes dietary, environmental and genetics.[4] The predominant pathophysiological features of HTN are microvascular rarefaction

Received: 10 July 2024
Accepted: 24 September 2024
Published: 2 October 2024

Graphical Abstract

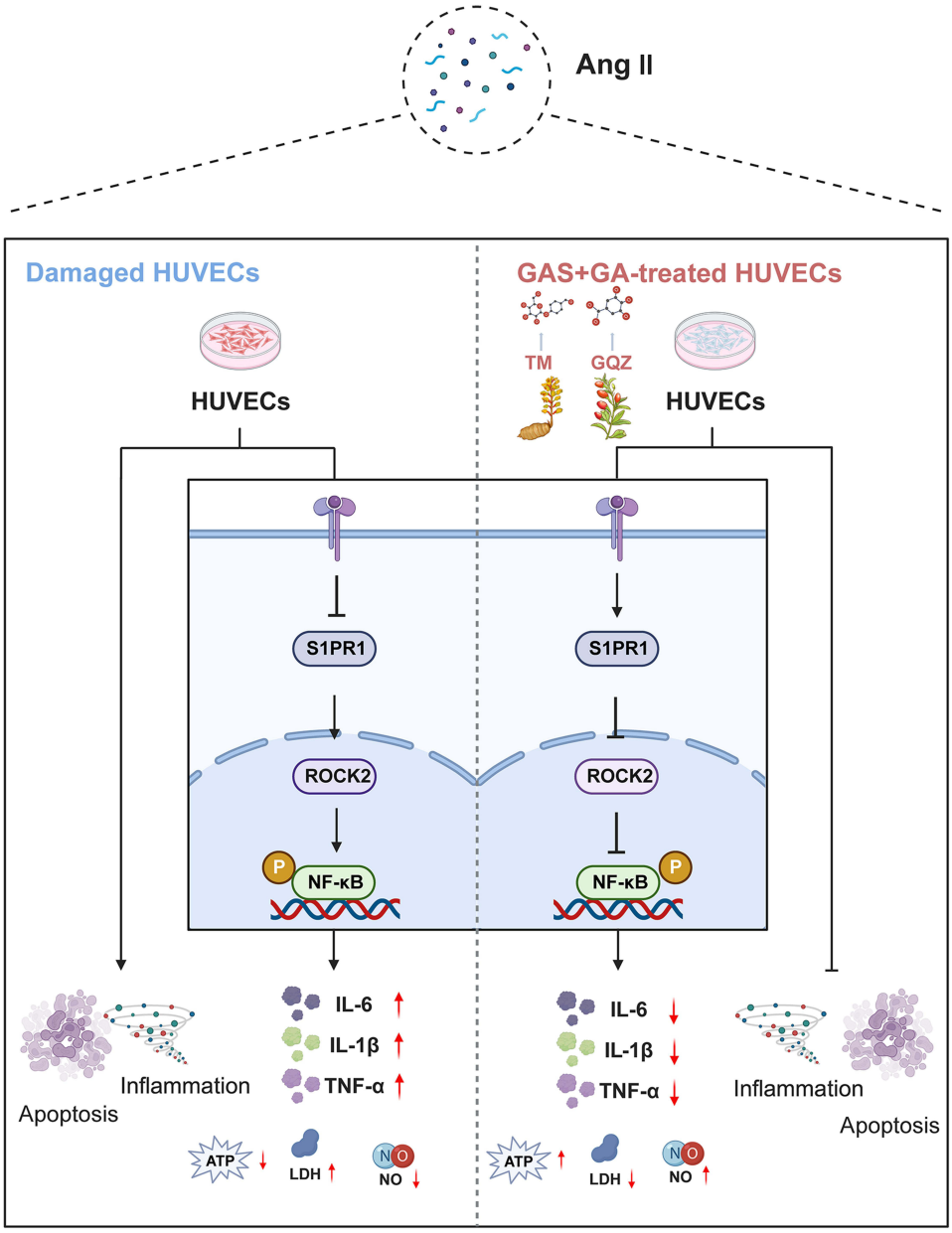

and endothelial dysfunction.[5] Clinical studies have shown that endothelial fibrinolysis induced by endothelial cell injury decreases in hypertensive individuals.[6]

Vascular inflammation is an early manifestation and the pathophysiological basis of HTN.[7] Endothelial cell-cell interactions shield tissues and organs from edema and unchecked infiltration of inflammatory cells, which are vital for vascular integrity and function.[8] Angiotensin II (Ang II) is the main bioactive peptide of the renin/angiotensin system, which causes oxidative stress, vascular inflammation, and cell apoptosis, leading to the dysfunction of vascular endothelial cells and is closely related to the occurrence and development of HTN.[9,10] Specifically, AngII could stimulate the production of thromboxane A2 (TXA2), endothelin 1 (ET-1), inducible nitric oxide synthase (iNOS), which increased platelet aggregation and vasoconstriction, elevated vascular permeability and promoted smooth muscle cell proliferation,

and contributed to the formation of peroxynitrite, respectively, exacerbating endothelial damage and promoting inflammatory responses.[11] Furthermore, an increase in inflammation and apoptotic cells further aggravates metabolic disorder.[12]

Sphingolipids are essential components of cell membranes and organelles that contribute to maintaining cell homeostasis and regulating cell development, differentiation, aging, and programmed cell death.[13] Furthermore, sphingolipids can retain endothelial cells in a normal state by providing conditions to maintain normal vascular tension, permeability, and oxidative stress responses.[14] When sphingolipid metabolism is disrupted, endothelial cells are inevitably injured, which leads to various cardiovascular disorders.[15] Therefore, the regulation of sphingolipid metabolism to inhibit inflammation and apoptosis of endothelial cells is expected to provide a new avenue for the treatment of HTN.

Gastrodiae Rhizoma is the dried tuber of *Gastrodia elata* Bl., of the family Orchidaceae called tianma (TM) in Chinese, a popular traditional medicine with a wide range of biological activities, including circulatory regulation, anti-inflammatory, anti-oxidant, anti-ageing, anti-viral, and anti-tumour effects.[16,17] Studies have shown that Gastrodiae Rhizoma can attenuate HTN and ameliorate hypertension-induced inflammation.[18] Lycii Fructus is the dried mature fruit of *Lycium barbarum* L. of the family Solanaceae, which is known in China as gouqizi (GQZ). Modern pharmacological studies have shown that GQZ has a variety of pharmacological effects, such as strengthening immunity, enhancing hypotensive action, improving memory, and suppressing tumor growth.[19] Studies have indicated that the polyphenolic compounds in GQZ, particularly GA, can not only alleviate hypertensive disease by dilating thoracic aortic vessels in both endothelium-dependent and non-endothelium-dependent manners,[20] but can also significantly reduce blood pressure in spontaneously hypertensive rats by inhibiting angiotensin-converting enzyme, and have comparable potency to the pharmacological effects of captopril.[21] However, whether regulating sphingolipid metabolism could inhibit the inflammation and apoptosis of endothelial cells and the underlying mechanisms remain unclear.

Human Umbilical Vein Endothelial Cells (HUVECs) are a widely accepted and well-established model for studying endothelial cell function and injury. They closely resemble the endothelial cells found in human blood vessels and are particularly useful for investigating mechanisms underlying vascular injury and inflammation.[22,23] HUVECs are known to exhibit characteristic responses to Ang II, such as increased oxidative stress, inflammation, and apoptosis.[11,24,25] This makes them a suitable model for assessing the protective effects of pharmacological agents against Ang II–induced endothelial damage.

In the current study, the integration of network pharmacology and molecular docking was initially used to explore the bioactive components, potential targets, and pathways of TM and GQZ in the treatment of HTN. The synergistic protective effects of gastrodin and gallic acid were evaluated in Ang II–induced Human umbilical vein endothelial cells (HUVECs) injury. Moreover, the Chou-Talalay model was used to assess synergistic effects, and the vital cell transduction pathway related to sphingolipids was experimentally verified by Western blot**ting** and molecular dynamics simulation. This study provides evidence for the elucidation of the synergistic effects of a combination of gastrodin and gallic acid from the perspective of sphingolipid metabolism in endothelial cells.

Materials and Methods

Materials

Human umbilical vein endothelial cells (HUVECs), DMEM medium, F12-K medium, penicillin/streptomycin solution, fetal bovine serum (FBS), the kits for measuring Nitric Oxide Content (NO), lactate dehydrogenase (LDH), interleukin-6 (IL-6), interleukin-1β (IL-1β), Tumor Necrosis Factor Alpha (TNF-α), Endothelin-1 (ET-1), Thromboxane B2 (TX-B2), inducible nitric oxide synthase (iNOS) and the secondary antibody for fluorescence were purchased from Sangon Biotech (Shanghai, China). The Annexin V-FITC apoptosis detection kit was purchased from Solarbio (Beijing, China). Gastrodin (GAS), 4-Hydroxybenzyl alcohol (PHE), Parishin A (PA), Lycium barbarum polysaccharides (LBP), luteolin (LUT), and gallic acid (GA) (purity ≥ 98%) were purchased from Jingzhu Biotech (Nanjing, China). The anti-Caspase-3 antibody and anti-cleaved caspase-3 antibodies were purchased from Cell Signaling Technology (USA). The anti-EDG1, anti-ROCK2, anti-phospho-NF-κB p65 (Ser536), and anti-β-actin antibodies were purchased from Bioss Biotech (Beijing, China). DNase/RNase-free Water, TransZol Up Plus RNA kit, all-in one first-strand cDNA synthesis SuperMix kit, and SYBR PCR Master Mix were purchased from TransGen (Beijing, China).

Compounds Screen and Targets Prediction

The bioactive compounds were identified using TCMSP, TCMIP, and SwissTarget Prediction database with the keywords "Gastrodiae Rhizoma" and "Lycii Fructus", and were filtered based on oral bioavailability (OB) ≥30% and drug-likeness (DL) ≥0.18. The bioactive compounds reported in the literature[26–29] were also collected. The bioactivity and relevance of these compounds based on their reported effects and interactions as documented in the literature. Furthermore, compounds, such as gastrodin and Lycium barbarum polysaccharide with clear pharmacological effects were chosen for additional investigation. SEA (https://sea.bkslab.org) and STITCH (http://stitch.embl.de) databases were used to screen the targets of these bioactive compounds. Genecards (https://www.genecards.org/), DisGeNET (https://www.disgenet.org/home/), OMIM (https://www.omim.org/), Malacard (https://previous.malacards.org/), and TTD (https://db.idrblab.net/ttd/) databases were used to search for hypertension-related targets. We employed search terms related to HTN, such as "hypertension", "high blood pressure", and assessed the relevance of each target by evaluating the strength of the evidence supporting its involvement in HTN. This included reviewing published literature, experimental validation, and known interactions with antihypertensive drugs.

Construction of Protein-Protein Interaction (PPI) Network

To better analyze the functional interaction between targets, the common targets of TM-GQZ and HTN were input into the STRING online platform (version 12.0) (https://string-db.org/), selected "Multiple proteins", and limited species to "Homo sapiens". We used a minimum interaction score of >0.400 to filter the results based on the strength of interaction evidence, as this threshold was chosen to balance between sensitivity and specificity in identifying meaningful interactions. The intersection targets were input into Cytoscape 3.7.2 software to construct the PPI, and Cytohubba was used to identify the densely connected network to screen the target correlation.

Enrichment Analysis

Common drug-disease targets were entered into the DAVID database (https://david.ncifcrf.gov/) for Gene Ontology (GO) and Kyoto Encyclopedia of Genes and Genomes (KEGG) pathway enrichment analysis. "Homo sapiens" was selected as the species. Biological processes (BP), cellular components (CC), and molecular functions (MF) were screened at $P<0.05$, and the obtained items were sorted according to the *P* value. The top 10 items were visualized using R software 3.4.1.

Molecular Docking

Molecular docking can effectively predict the possibility of a compound binding to a target. AutoDock-Vina software was used for semi-flexible docking. Semi-flexible docking offers a balance of efficiency and accuracy by allowing ligand flexibility while keeping the protein rigid, which is computationally less demanding than fully flexible docking. The top five target proteins in the above analysis were verified by molecular docking with the core active components. The 3D structure of the target protein and chemical structures of GAS, PHE, PA, LBP, LUT, and GA were obtained from the RCSB PDB protein database (https://www.rcsb.org/) and PubChem database (https://pubchem.ncbi.nlm.nih.gov/), respectively, the details of structure IDs which are available in Supplementary Tables 1 and 2. AutoDock Tools software was used to prepare input files, set docking parameters, and analyze results for our protein-ligand simulations, and the Autogrid plug-in was used to obtain the docking active sites for molecular docking to determine the affinity. Here, we used PyMOL v.0.99 software to visualize the 3D structures of docking results.

Cell Culture and Drug Treatment

The HUVECs were seeded with 1.2×10^5 cells/mL and cultured in F-12K Medium containing 10% FBS, 0.1 mg/mL heparin, and 30 μg/mL ECGS at 37 °C with 5% CO_2.[30] GAS, PHA, PA, LBP, LUT, and GA were dissolved in DMSO at concentrations of 100 mg/mL. The cells were treated with 1 μM Ang II for 12 h and then treated with the above compounds.

Cell Viability Assay

HUVECs were grown in 96-well plates at a density of 1.2×10^4 per/well. After the cells were treated as described above, the supernatant was discarded and the cells were treated with MTT for 4 h. Subsequently, DMSO was added, and the absorbance was recorded at 570 nm using a microplate reader (Tecan, CH).[31]

Cell Morphology Observation

HUVECs were seeded in 6-well plates at a density of 1.8×10^5 cells per well. After treatment as described above, morphological changes in the cells were visualized using a microscope (Nikon, Japan).

Evaluation of the Synergistic Effect

The hypotensive effects of GAS and GA were tested at concentrations of 0.8, 4, 20, and 100 μM and 0.16, 0.8, 4, and 20 μM. The combination doses were determined based on the optimal hypotensive effects of the treatment groups. Sixteen combinations of GAS and GA were used to determine the optimal synergistic dose and dose range. The combination treatment cell viability results were further analyzed using the Chou-Talalay model to determine the synergistic effect. Chou-Talalay model analysis was performed using CompuSyn software.[32] The CompuSyn program was used to compute the combination index (CI) for the studied drug combinations. The resulting CI offers a quantitative definition of the additive effects (CI = 1), synergism (CI < 1), and antagonism (CI > 1) in drug combinations.[33] The optimal synergistic combination dose and single dose were used in subsequent experiments to identify possible synergistic hypotensive effect mechanisms.

NO, LDH, IL-6, IL-1β, TNF-α, ET-1, TX-B2, iNOS Measurement

HUVECs were treated as described above. After drug treatment, the supernatants were collected. The levels of NO and LDH were measured using commercial kits according to the manufacturer's instructions. The secretion of IL-6, IL-1β, and TNF-α was detected using qPCR and ELISA kits following the manufacturer's instructions. The expression level of ET-1, TX-B2, iNOS was measured using ELISA kits following the manufacturer's instructions. The OD values were recorded at 450 nm, and the levels of IL-6, IL-1β, and TNF-α, Thromboxane A2 and iNOS were found to be directly proportional to the OD values. The concentrations of IL-6, IL-1β, and TNF-α, ET-1, TX-B2, iNOS were determined using a standard curve.[34]

Annexin V-FITC/PI Staining

Apoptotic cells were analyzed using Annexin V-FITC/PI staining.[35] The cells were harvested and incubated with Annexin V-FITC/PI (1×) working solution for 15 min. Apoptotic cells were quantified using a FACSCalibur II flow cytometer (BD Biosciences).

qRT-PCR Analysis

The primers were synthesized by Sangon Biotech (Shanghai, China), and the sequences are shown in Supplementary Table 3. Total RNA from T98G cells was extracted and reverse-transcribed to cDNA using PrimeScript™RT Master Mix and TB Green® Premix Ex Taq™ II. Relative mRNA expression was analyzed using the $2^{-\Delta\Delta Ct}$ method as described previously.[36]

Western Blot Analysis

After drug treatment and cell sampling, Western blotting was performed to detect the expression of BAX, BCL-2, S1PR1, ROCK2, and p-NF-κB. The cells were lysed to obtain protein lysates. Equal amounts of protein were separated by 10% electrophoresis and transferred onto PVDF membranes. After sealing with 5% skim milk, primary and secondary antibodies were used for the analysis.[37] Finally, the proteins were scanned using a ChemiDocTM XRS+ system (Bio-Rad, USA) and analyzed using the ImageJ software.

Molecular Dynamics Simulation

Molecular dynamics simulations (MD) were conducted using the GROMACS 2022 [38] program with constant temperature, pressure, and periodic boundary conditions. The proteins obtained from the docking results were separated from the best small

molecule ligands, the details of structure IDs which are available in Supplementary Tables 1 and 2. Small-molecule force field files were generated using the antechamber tool in Ambertools software and then converted to gromacs force field files using the Acpype software tool. The simulation system for the complex was created by combining the protein and small-molecule ligand files. The GAFF force field was used for small molecules, whereas the AMBER14SB force field and TIP3P water model were used for proteins. The LINCS algorithm was employed to constrain all hydrogen bonds, with an integration step of 2 fs. Electrostatic interactions were calculated using the Particle-mesh Ewald (PME) method, with a cutoff value of 1.2 nm. The cutoff for non-key interactions was set to 10 Å and updated every 10 steps. The temperature was maintained at 298 K using the V-rescale temperature-coupling method, whereas the pressure was maintained at 1 bar using the Berendsen method. Equilibrium simulations were conducted at 298 K for 100 ps using the NVT and NPT. MD simulations were then performed for 100 ns on the complex system, with conformations saved every 10 ps. Finally, the simulated trajectories were analyzed using VMD and PyMOL.

Statistical Analysis

Statistical analysis was performed using one-way analysis of variance (ANOVA) followed by Dunnett's test and is presented as mean ± SEM (GraphPad Prism 8.0). * $p < 0.05$, ** $p < 0.01$, *** $p < 0.001$, **** $p < 0.0001$ were defined as statistically significant.

Results

Screening of Major Bioactive Components and Construction of the Anti-Hypertension Targets Network of TM-GQZ

To explore the therapeutic mechanism of TM-GQZ in the treatment of HTN, 3302 disease-related targets were initially identified (Figure 1A) he details of which are available in Supplementary Table 4. Furthermore, the Venn diagram indicated 133 and 202 targets for TM and GQZ, respectively, in the treatment of HTN, the details of which are available in Supplementary Table 5. The combination of TM and GQZ resulted in 39 shared targets for the treatment of HTN (Figure 1B), the details of which are available

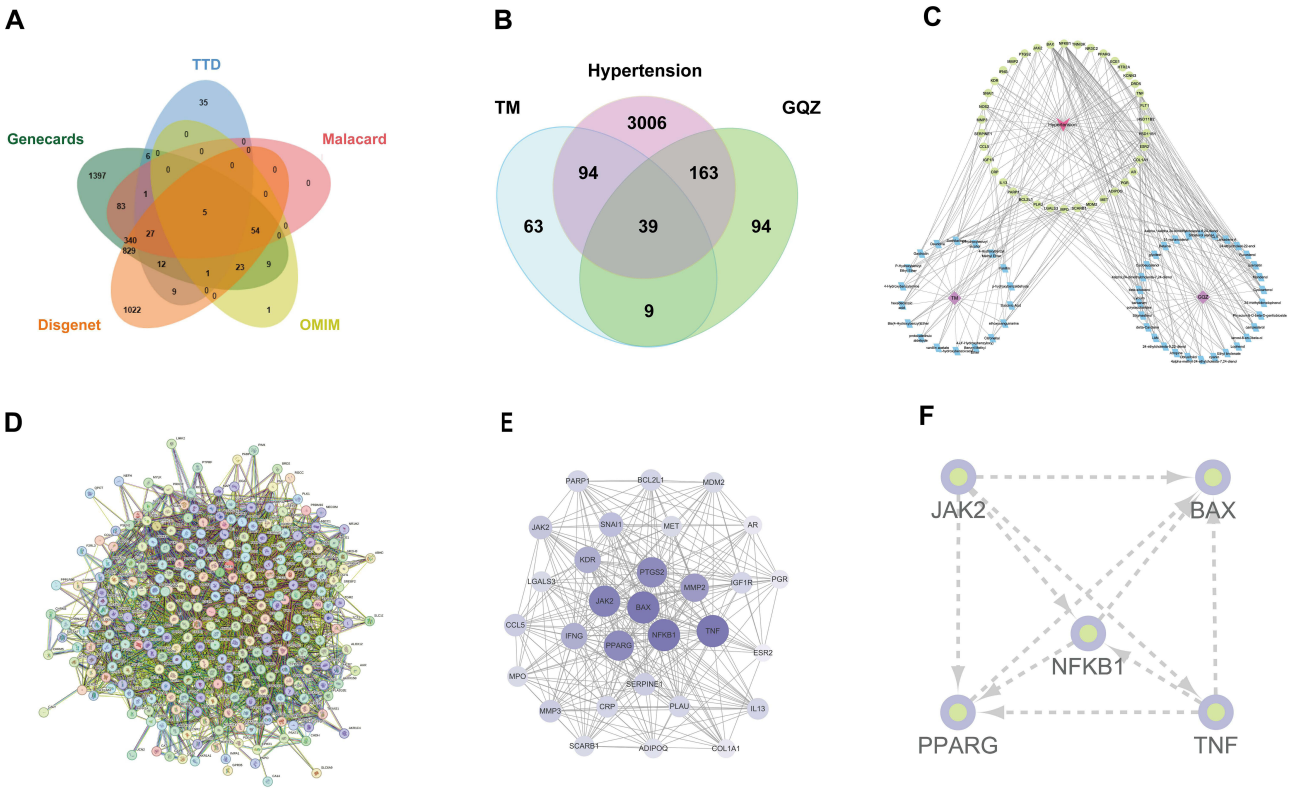

Figure 1 The network construction and topological analysis of anti-hypertension targets of TM-GQZ. (**A** and **B**) Venn analysis of hypertension-related targets (**A**) and common targets of TM-GQZ in treating hypertension (**B**). (**C**) Compound-target network of TM-GQZ. (**D**) The PPI network construction of the common targets. (**E**) The construction of sub-network. (**F**) The construction of interaction network of key targets.

in Supplementary Table 6. 18 active compounds of TM and 29 active compounds of GQZ were selected using OB and DL filtering criteria. Comprehensive details about these active ingredients can be found in Supplementary Table 7. The drug-compound-target network was constructed using Cytoscape (Figure 1C). Through degree ranking, GAS, PHE, PA, LBP, LUT, and GA were selected as important bioactive compounds for further verification. The antihypertensive targets of TM-GQZ were imported into the STRING database to obtain a protein-protein interaction network (Figure 1D). The interaction network was analyzed using the MCODE plug-in of Cytoscape software, and the subnetwork with the highest MCODE score was obtained (Figure 1E). In the subnetwork, the top five targets with larger weights, including NF-κB1, JAK2, BAX, PPARG, and TNF, may be the key targets for TM-GQZ to exert antihypertensive effects. (Figure 1F).

Biological Processes and KEGG Pathways Affected by TM-GQZ in Treating HTN

To explore the functional annotation of the targets regulated by TM-GQZ in the treatment of HTN, GO and KEGG enrichment analysis was performed with the "clusterProfiler" package (v. 4.4.4) with a p-value threshold set to 0.05. The results revealed that these targets were mainly enriched in the inflammatory response and apoptotic process (Figure 2A),

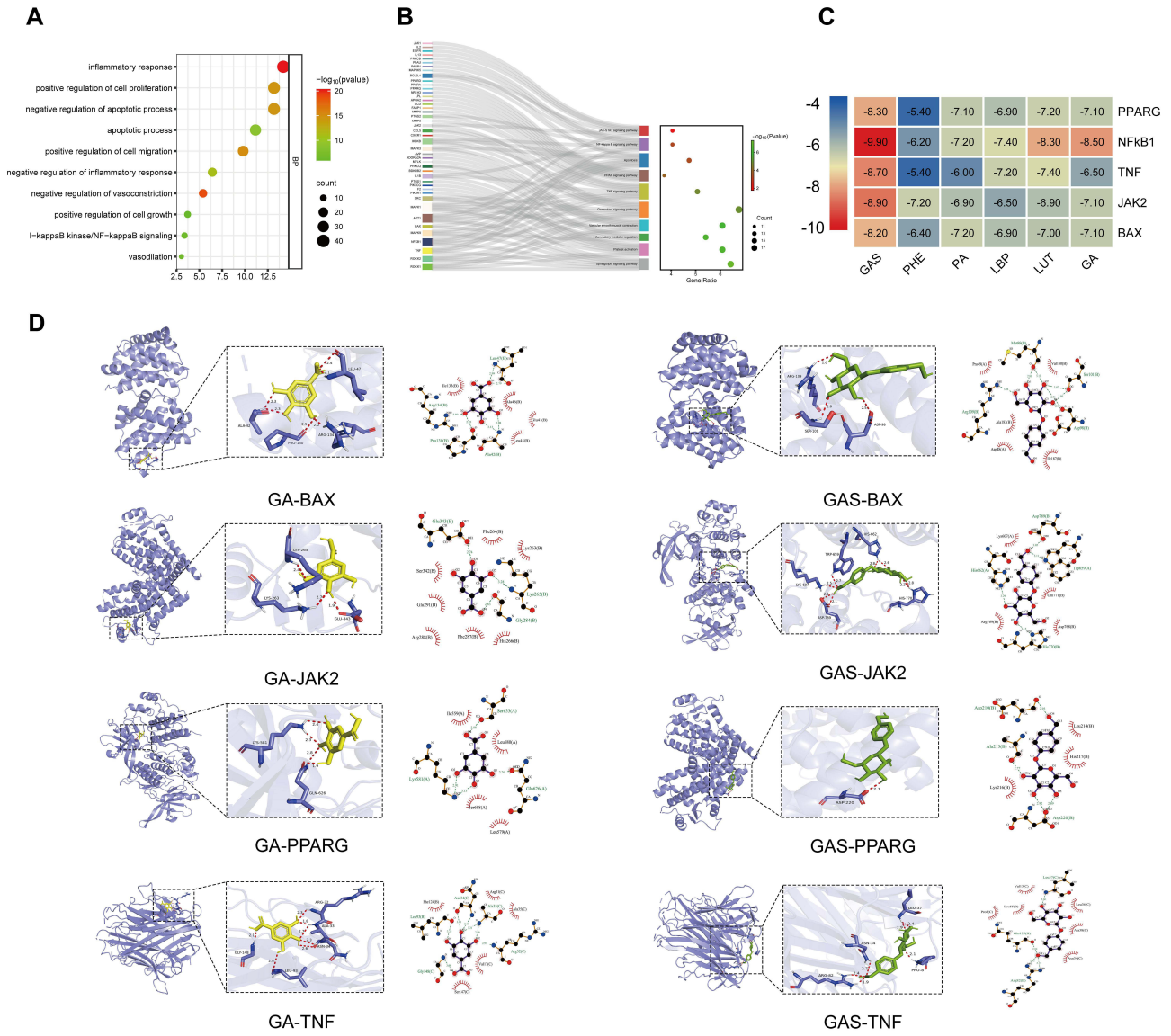

Figure 2 The enrichment analysis and molecular docking. (**A** and **B**) Biological process analyses (**A**) and KEGG pathway analyses (**B**) of common targets of TM-GQZ in treating hypertension (p-value < 0.05). (**C**) The docking scores of key active components of TM-GQZ with the five hub targets. (**D**) Three-dimensional visual representation and two-dimensional visual representation of the molecular docking interactions between active ingredients and hub targets.

indicating that inflammation and apoptosis are both important biological events that are altered during HTN. Furthermore, KEGG pathway analysis showed that multiple inflammation-related, apoptosis-related, and sphingolipid signaling pathways were highly enriched (Figure 2B).

Molecular Docking Results

To further explore the possible binding modes between the active components (GAS, PHE, PA, LBP, LUT, and GA) and hub genes (PPARG, NF-κB1, TNF, JAK2, and BAX), binding affinities were predicted using AutoDock Vina. Binding stability between receptors and ligands is governed by their binding energy. A lower binding energy signifies greater stability in the receptor-ligand conformation.[39,40] Consequently, we identified the most effective ligand (having the lowest binding energy) for receptor binding, using binding energy as the primary criterion. As shown in Figure 2C, the results showed that the binding energies of hub genes with key active components. Figure 2D, Figure 7A and B illustrated the interactions between the receptors and ligands. Among them, GA bound to BAX through 6 hydrogen bonds formed by ALA-42, PRO-130, ARG-134, and LEU-47, GA bound to JAK2 through 3 hydrogen bonds formed by LYS-263, LYS-265 and GLU-343, GA bound to PPAARG through 4 hydrogen bonds formed by LYS-518, GLN-626, GA bound to TNF through 7 hydrogen bonds formed by GLY-148, LEU-93, ASN-34, and ALA-33, ARG-32, GA bound to NF-κB1 through hydrogen bond formed by ARG-156, GAS bound to BAX through 7 hydrogen bonds formed by LYS-607, ASP-789, HIS-770 and HIS-662, GAS bound to JAK2 through 3 hydrogen bonds formed by LYS-263, LYS-265, GLU-343, GAS bound to PPAARG through hydrogen bond formed by ASP-220, GAS bound to TNF through 6 hydrogen bonds formed by ASN-34, ARG-82, PRO-8, and LEU-37, GAS bound to NF-κB1 through 5 hydrogen bonds formed by ASN-138, ALA-137 and LEU-69. The above results indicated that these five components can bind well with these two proteins.

AngII Induces Cytotoxicity and Injury of HUVECs

The physiological function of endothelial cells play an important role in maintaining normal cardiovascular functions. Ang II–induced endothelial dysfunction is a pathological mechanism underlying the occurrence and development of cardiovascular disease. MTT results showed that 0.1 μM and 1 μM AngII markedly reduced cell viabilities as compared with control group, and 1 μM AngII decreased the cell viability by 39.83% (Figure 3A). Furthermore, the results revealed

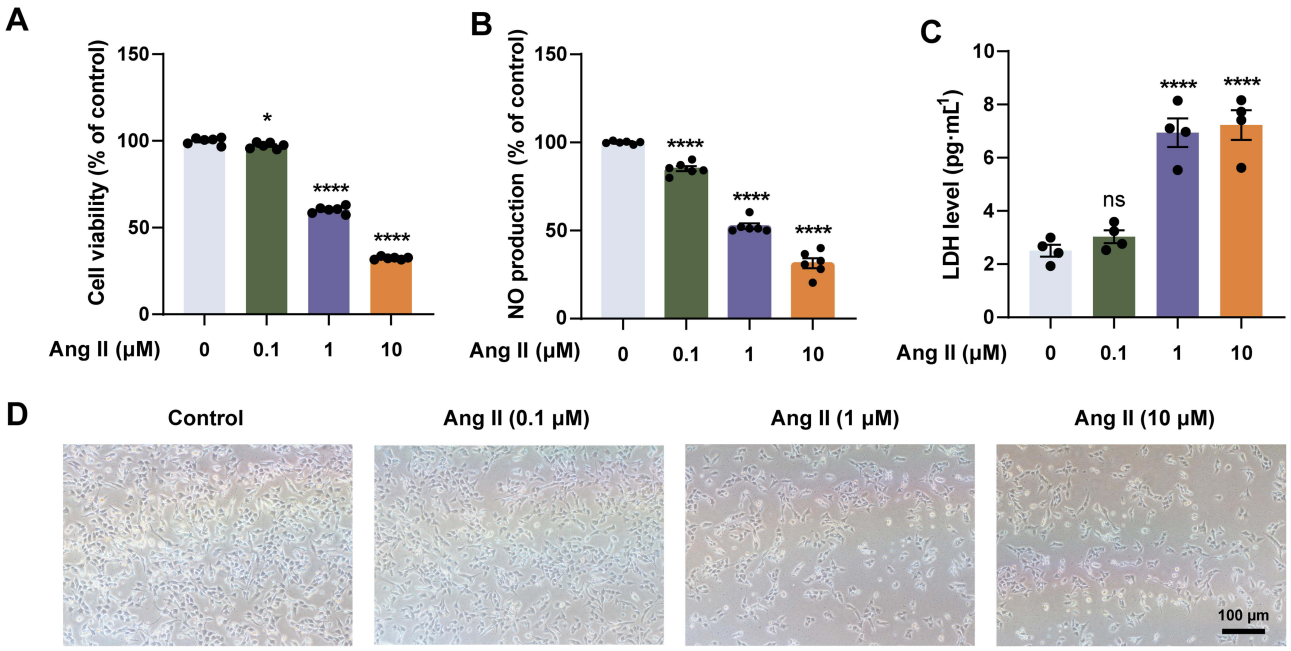

Figure 3 Ang II induces cytotoxicity in HUVECs. (**A**) Viability of HUVECs incubated with 0, 0.1, 1, and 10 μM Ang II for 12 h (n=6). (**B**) NO release in HUVECs stimulated with 0, 0.1, 1, and 10 μM Ang II for 12 h (n=6). (**C**) LDH levels of HUVECs treated with 0, 0.1, 1, or 10 μM Ang II for 12 h (n=6). (**D**) Morphological changes in HUVECs treated with 0, 0.1, 1, and 10 μM Ang II for 12 h (n=5). Scale bar, 100 μm. *P < 0.01, ****P < 0.0001 vs control group. Data are expressed as the mean ± SEM. Statistical significance was determined using one-way ANOVA for multiple comparisons. All experiments were repeated at least three times.

that 1 μM Ang II significantly decreased NO production and promoted LDH release (Figure 3B and C). Furthermore, inverted microscopy revealed that the cells in the control group were well-grown, numerous, with tight intercellular connections, polygonal or pike-shaped, uniform in size, and with clear boundaries. Compared with the control group, the number of cells in the model group after Ang II intervention was significantly reduced, the cells were less connected to each other, disorderly arranged, unevenly distributed in size, and the phenomenon of detachment was obvious. This was particularly evident in the HUVECs after 1 μM and 10 μM Ang II treatment (Figure 3D), suggesting that 1 μM Ang II induced injury in HUVECs, the concentration of which was chosen for the follow-up experiments.

The Protective Effects of Bioactive Components in AngII-Induced HUVECs

To investigate the effects of GAS, PHE, PA, LBP, LUT, and GA on HUVECs and Ang II-treated HUVECs, a cell viability assay was performed. The results demonstrated that GAS, PA, LBP, LUT, and GA were not cytotoxic to the HUVECs (Figure 4A–F). However, 20 and 100 μM PHE had slight toxic effects on HUVECs (Figure 4B). Moreover, MTT assay showed that GAS (0.8, 4, 20, 100 μM), PHE (100 μM), PA (100 μM), LBP (40, 200 μg/mL), LUT (10, 50 μM) and GA (0.8, 4, 20 μM) significantly increased cell viabilities of AngII-induced HUVECs (Figure 4G–L), and the effect of GAS and GA are significantly higher than other four components.

The Synergistic Effect of GAS and GA Based on Chou-Talalay Algorithm

Thus, a combination of GAS and GA may have synergistic effects. For this purpose, Ang II-treated HUVECs were treated with the indicated concentrations of GAS and GA, alone or in combination, and cell viability was measured using an MTT assay. The result revealed that The synergistic dose range was 4–100 μM GAS and 0.8–20 μM (Figure 5A). CI values were measured using the CompuSyn software. CI < 1.0 for virtually all conditions (except for one condition for the GAS and GA combination) indicated synergism between GAS and GA (Figure 5B), and the optimal synergistic dose was 20 μM of GAS and 4 μM of GA (Figure 5C). These results revealed that the combination of GAS and GA exerted synergistic effects. Thus, the concentrations of 20 μM GAS and 4 μM GA were chosen for subsequent studies.

The Synergistic Effect of GAS and GA on Inhibiting Inflammation and Apoptosis in AngII Induced HUVECs

To validate the synergistic anti-inflammatory and anti-apoptotic effects of GAS and GA, the production of NO, LDH leakage, the level of ET-1, iNOS and TX-B2, inflammatory cytokine secretion, apoptotic cell rate, and BAX and BCL-2 expression levels were measured. When cells were stimulated with 1 μM Ang II, the expression level of NO was significantly reduced by 64.80%. LDH release was markedly increased by 132.30% (Figure 6B), the ATP level was notably reduced by 56.95% (Figure 6C). The expression level of ET-1, iNOS, TX-B2 were notably increased by 133.90%, 109.61%, 255.11%, respectively (Figure 6D–F), the secretion of inflammatory cytokines (IL-6, IL-1β, TNF-α) was significantly increased (Figure 6G–I), the apoptotic cell rate was notably increased (Figure 6M–N), the expression of pro-apoptotic marker BAX was upregulated by 103.54%, and the protein level of anti-apoptotic marker BCL-2 was downregulated by 66.30% (Figure 6O–Q).

However, treatment with GAS (20 μM) and GA (4 μM) markedly increased NO levels by 90.21% and reduced LDH leakage by 53.33%. Meanwhile, treatment with GAS and GA elevated the ATP levels by 106.28%. Furthermore, combination of GAS and GA significantly decreased the expression level of ET-1, iNOS, TX-B2 by 44.12%, 38.68%, and 49.61%, respectively. qPCR and ELISA results showed that the combination of GAS (20 μM) and GA (4 μM) significantly decreased the levels of inflammatory cytokines (IL-6, IL-1β, and TNF-α). Moreover, the combination of GAS and GA markedly decreased the rate of apoptosis, downregulated BAX expression by 46.55%, and up-regulate the expression of BCL-2 by 186.33%. These results demonstrated that the combination of GAS and GA significantly alleviated Ang II–induced inflammation and apoptosis in HUVECs, the details of which are available in Supplementary Table 8.

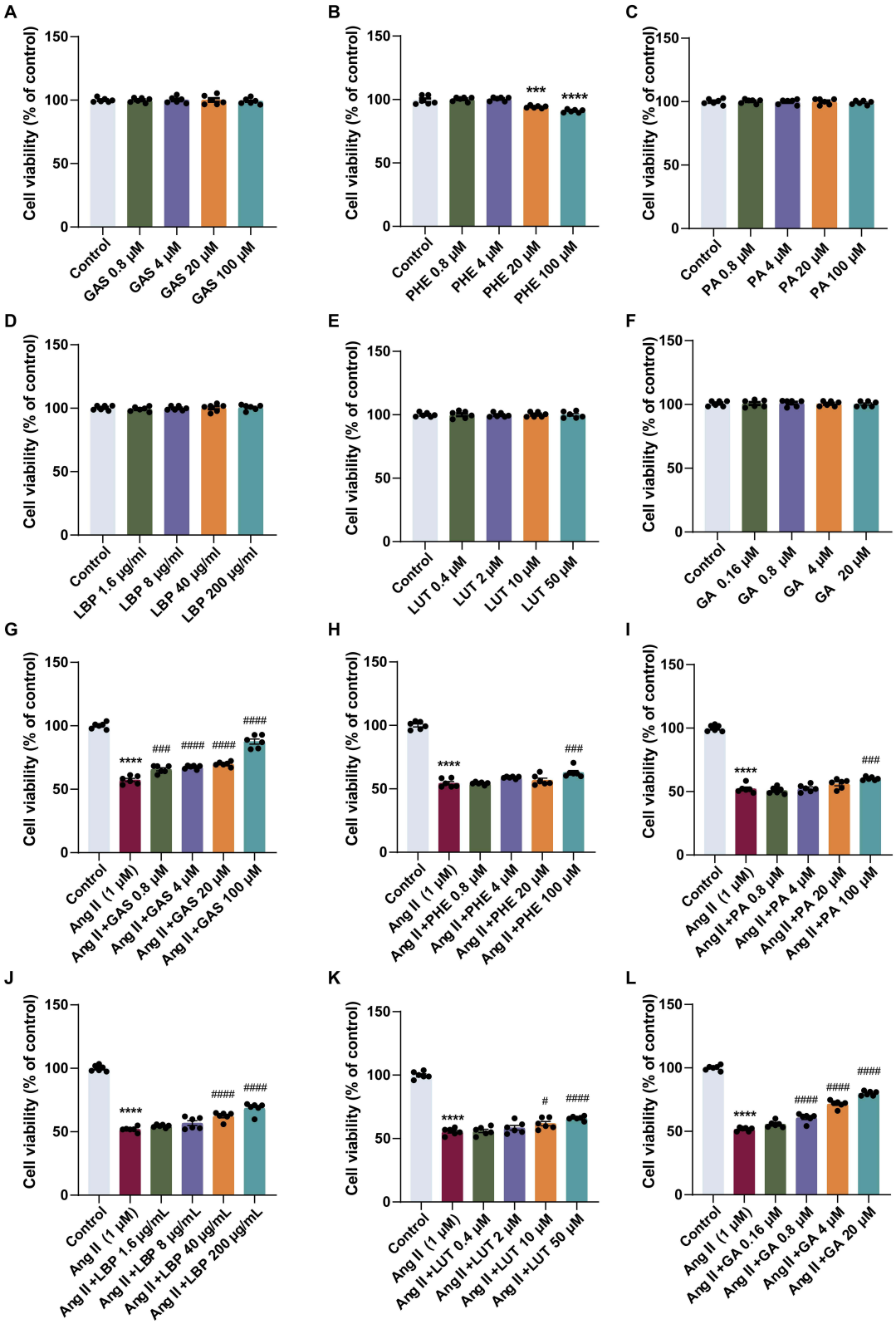

Figure 4 Protective effects of GAS, PHE, PA, LBP, LUT and GA on AngII-induced HUVECs. (**A-F**) Effects of GAS, PHE, PA, LBP, LUT and GA on cell viability of HUVECs (n=6). (**G-L**) Effects of GAS, PHE, PA, LBP, LUT and GA on cell viability of AngII-induced HUVECs (n=6). ***P < 0.001, ****P < 0.0001 vs control group. $^{\#}$P < 0.05, $^{\#\#\#}$P < 0.001, $^{\#\#\#\#}$P < 0.001 vs AngII group. Data were expressed as mean ± SEM. Statistical significance was determined by one-way ANOVA for multiple comparisons. Six replicates of each sample were subjected to an independent experiment, and the experiment was repeated six times.

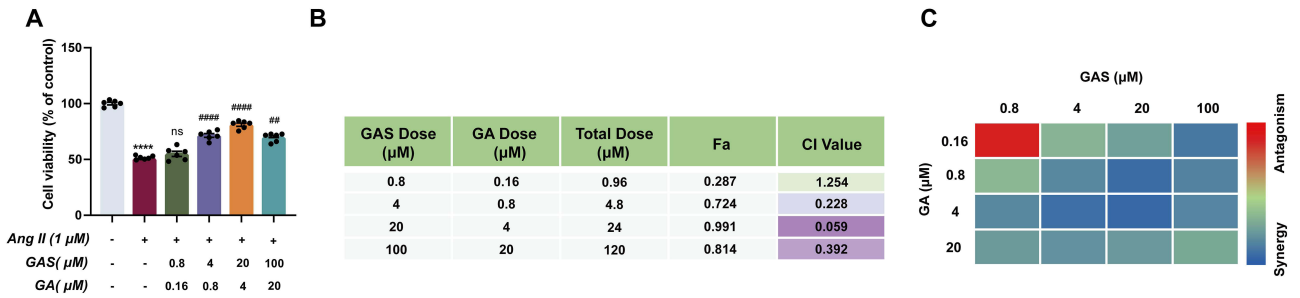

Figure 5 The synergistic neuroprotection effect of GAS and GA. (**A**) Effects of GAS and GA on cell viability of AngII-induced HUVECs (n=6). (**B** and **C**) Synergy analysis based on Chou-Talalay model (CI < 1.0, = 1.0, and > 1.0, indicating synergistic, additive, and antagonistic effect, respectively). ****P < 0.0001 vs control group. ##P < 0.01, ####P < 0.001 vs AngII group. ns, not significant. All data were shown as mean ± SEM. Statistical significance was determined by one-way ANOVA for multiple comparisons. All experiments were repeated independently for six times.

The Anti-Inflammatory and Anti-Apoptotic Effects of GAS and GA Combination Regulated by Sphingolipid Metabolism

To explore the potential mechanisms of the GAS and GA combination on sphingolipid suppression, the binding of GAS or GA with NF-κB1 was predicted by molecular dynamics simulations, and the protein levels of S1PR1, ROCK2, and p-NF-κB were detected by Western blotting in Ang II-treated HUVECs. Molecular docking results showed that amino acids ASN-138 and LYS-79 in NF-κB1 form hydrogen bonds with GAS, PRO-70, and LYS-79 from Pi-Alkyl and Pi-Cation hydrophobic interactions with GAS, and amino acids LYS-76 and TYR- 81 form van der Waals force interactions with GAS. Amino acids ILE-122 and ALA-160 in NF-κB1 formed Pi-alkyl hydrophobic interactions with GA, ARG-156 formed a salt bridge with GA, and amino acids VAL-97 and TYR-165 formed van der Waals interactions with GA (Figure 7A-B). The VDW for GAS, GA, and NF-κB1 binding was more stable relative to the ELE, and the binding between small molecules and proteins remained stable as the simulation progressed for GAS, GA, and NF-κB1 binding (Figure 7C and D). The number of hydrogen bonds between GAS and NF-κB1 was more stable, fluctuating mainly between one and five. The number of hydrogen bonds between GA and NF-κB1 was mainly below two after 30 ns, and the number of hydrogen bonds between small molecules and proteins was lower (Figure 7E and F). The RMSD of NF-κB1, the RMSD of the GA and NF-κB1 binding complex, and the RMSD of GAS and NF-κB1 binding remained stable after 50 ns. (Figure 7G and H). The Rg values of the complexes bound by GAS, GA, and NF-κB1 stabilized progressively during the simulation (Figure 7I and J). The distance between GAS and the initial binding site appeared to change before 50 ns (Figure 7K); however, analysis of its conformation (Figure 7M) revealed that the GAS small molecule moved near the initial binding site and stably bound to the initial binding site of NF-κB1 after 50 ns. The distance between GA and the initial binding site, the docking site, changed in a stepwise manner (Figure 7L), and the trajectory of the small molecule was analysed (Figure 7N), which showed that GA moved on the surface of NF-κB1 from the initial binding site at 0 ns to the site at 50 ns, and then to the 100 ns site, which were all close to the initial binding site, and the distance between GA and the centre of the NF-κB1 protein did not change by more than 2 nm.The Buried SASA for GAS binding to NF-κB1 remained stable after 50 ns (Figure 7O). The Buried SASA for GA binding to NF-κB1 fluctuated in accordance with the distance between GA and NF-κB1, with the highest Buried SASA at the initial binding site (Figure 7P). The superimposed conformations of GAS, GA, and NF-κB1-bound GAS were located near the initial binding site (Figure 7Q and R). The major conformations of GA and NF-κB1-bound GA were distributed in three positions, corresponding to the three sites previously analyzed for the binding of GA small molecules to NF-κB1. The above results indicated that when GAS and NF-κB1 are combined, van der Waals interactions play a major role, electrostatic interactions play a minor role, and hydrophobic interactions play a complementary role.When both GA and NF-κB1 are combined, electrostatic interactions play a major role, van der Waals interactions play a minor role, and hydrophobic interactions play a complementary role. GAS or GA with NF-κB1 combined with Good stability, high binding energy and affinity.

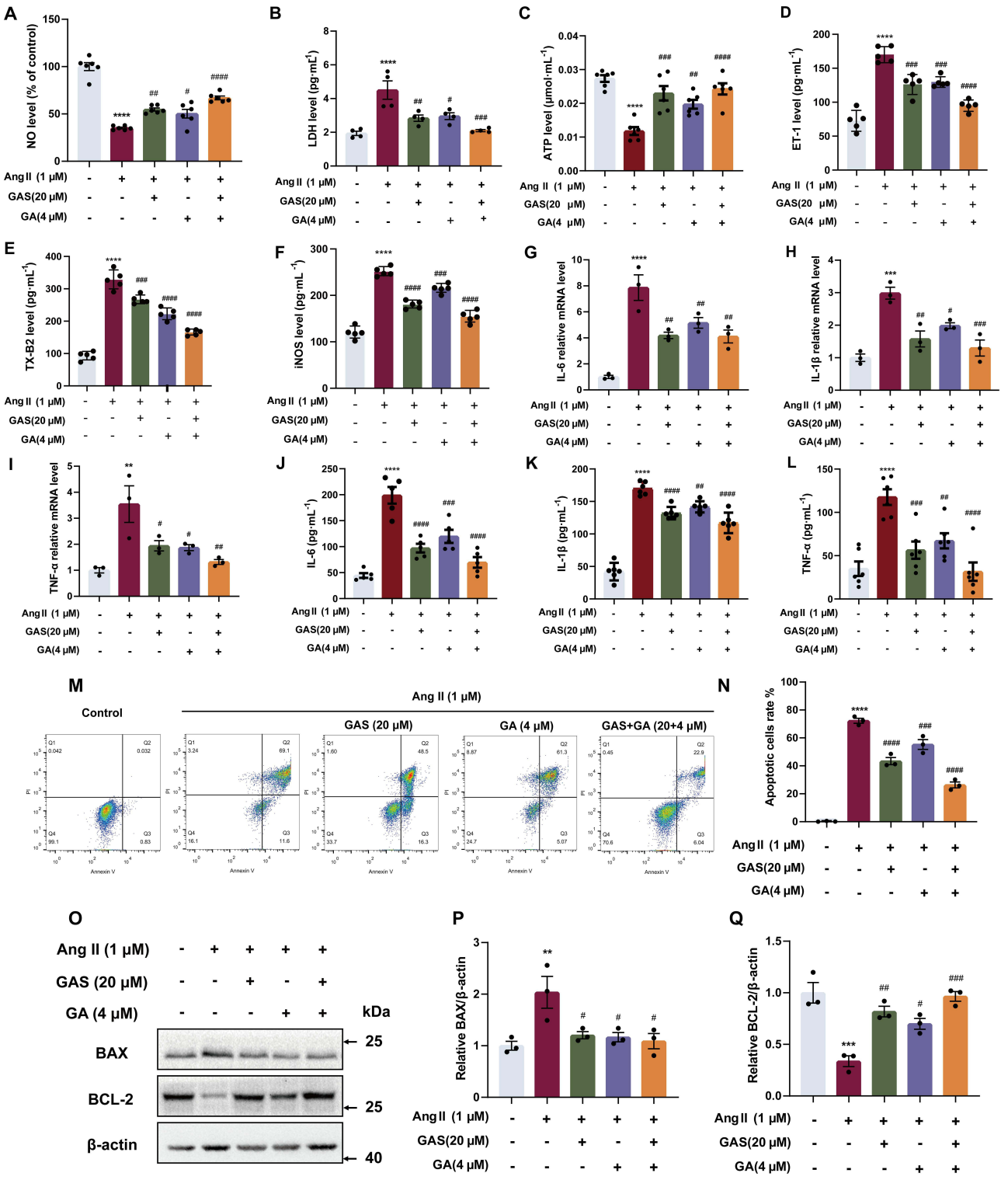

Figure 6 The effects of GAS and GA combination on inflammation and apoptosis. (**A**) The NO production (n=6). (**B**) The LDH leakage (n=4). (**C**) The ATP level (n=6). (**D**) The ET-1 level (n=5). (**E**) The TX-B2 level (n=5). (**F**) The iNOS level (n=5). (**G–I**) The mRNA expression of IL-6, IL-1β and TNF-α detected by qPCR (n=3). (**J–L**) The secretion of IL-6, IL-1β and TNF-α detected by ELISA assay (n=4). (**M** and **N**) The effects of GAS and GA combination on apoptotic cells rate (n=3). (**O–Q**) The expression of BAX and BCL-2 (n=3). **P < 0.01, ***P < 0.001, ****P < 0.0001 vs control group. #P < 0.05, ##P < 0.01, ###P < 0.001, ####P < 0.0001 vs AngII group. All data were shown as mean ± SEM. Statistical significance was determined by one-way ANOVA for multiple comparisons. All experiments were repeated independently at least three times.

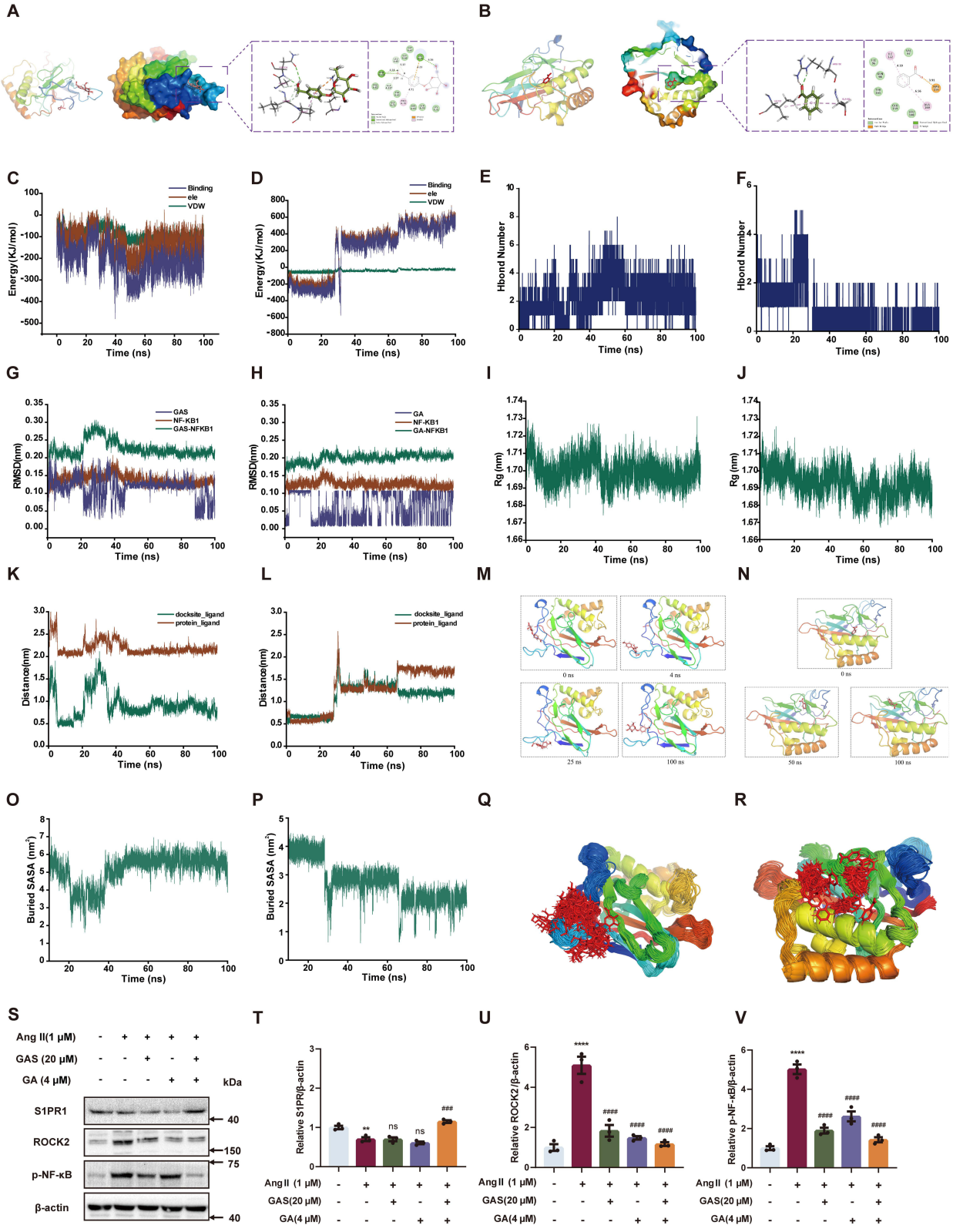

Figure 7 Sphingolipid metabolism is involved in the anti-inflammatory and anti-apoptotic effects of GAS and GA combination. (**A** and **B**) The simulated binding conformations of GAS, GA binding with NF-κB separately. (**C** and **D**) The van der Waals and electrostatic interactions between GAS, GA and NF-KB. (**E** and **F**) The Hbond number of GAS and GA to NF-κB. (**G**–**J**) The RMSD, Rg results of GAS, GA binding with NF-κB separately. (**K** and **L**) The Dock Site-ligand for the binding site of GAS, GA binding with NF-κB separately. (**M** and **N**) The binding trajectories of GAS, GA binding with NF-κB separately. (**O** and **P**) The Buried SASA of GAS, GA binding with NF-κB separately. (**Q** and **R**) The Simulated conformational superposition of GAS and GA to NF-κB. (**S**–**V**) The protein level of S1PR1, ROCK2 and p-NF-κB (n=3). $^{**}P < 0.01$, $^{****}P < 0.0001$ vs control group. $^{\#\#\#\#\#}P < 0.001$, $^{\#\#\#\#\#}P < 0.001$ vs AngII group. ns, not significant. All data were shown as mean ± SEM. Statistical significance was determined by one-way ANOVA for multiple comparisons. All experiments were repeated at least three times.

Western blotting showed that 1μM AngII II decreased S1PR1 expression by 29.83% and notably increased the protein levels of ROCK2 and p-NF-κB by 409.87% and 402.31%, respectively. However, treatment with GAS (20 μM) and GA (4 μM) markedly elevated S1PR1 levels by 63.91% (Figure 7S and T), and suppressed the expression of ROCK2 and p-NF-κB by 77.08% and 71.53% (Figure 7S, U and V). The above results revealed that the combination of GAS and GA could regulate the protein levels of S1PR1, ROCK2, and p-NF-κB in Ang II-treated HUVECs, which are the key targets participating in sphingolipid metabolism.

Discussion

HTN continues to pose a major hazard to human health, and has emerged as a high-incidence disease. Current treatment for HTN includes medications such as diuretics and ACE inhibitors, as well as lifestyle changes like diet, exercise, and weight management. However, there is no cure for HTN at present.[41] Numerous studies have demonstrated the effectiveness of Chinese medicine may be in treating HTN.[42] Chinese herbal formulas are frequently used in the clinical practice. Compounding enables drug interactions, which can result in a series of biochemical reactions that enhance efficacy and decrease toxicity.[43,44] The compatibility concept of traditional Chinese medicine is based on experience, but its potential interactions and mechanisms are yet to be elucidated.

Studies have demonstrated the beneficial antihypertensive effects of TM and GQZ; however, the precise active chemical components and associated mechanisms remain unknown.[27,28,45,46] Specifically, TM and GQZ contain substances, such as polyphenols and polysaccharides, which are the main biologically active compounds with antihypertensive properties.[28,47,48] The polyphenolic components in the GAS and gallic GA formulations have been the most widely studied for their antihypertensive activity.[26,27,49,50] Therefore, GAS and GA are the primary active components of TM and GQZ, respectively, both of which have antihypertensive effects. Nonetheless, the antihypertensive mechanisms of TM and GQZ remain unknown; thus, network pharmacology could help identify key targets. The topology-based network analysis revealed that GAS, PHE, PA, LBP, LUT, and GA were the main active components. Moreover, the top five targets with the greatest weight, including NF-κB1, JAK2, BAX, PPARG, and TNF, were considered potential targets for the compatibility of TM and GQZ.

Recent studies have shown that GAS reduces inflammation by inhibiting the NF-κB pathway and enhancing antioxidant defenses, while GA modulates inflammation by suppressing pro-inflammatory cytokines and MAPK pathways.[51] Both substances lower blood pressure by improving endothelial function and inhibiting angiotensin-converting enzyme activity.[52–54] Additionally, GAS and GA counteract atherosclerosis by improving lipid profiles, reducing oxidative stress, and enhancing endothelial health.[55,56] These findings align with recent literature and highlight the synergistic potential of these substances in managing inflammation, HTN, and atherosclerosis. The results of our current study revealed that GAS and GA synergistically protected HUVECs from Ang II–induced injury. Ang II plays a critical role in the inflammatory cascade by inducing vasoconstriction, promoting atherosclerosis, and contributing to cardiovascular events.[57] It elevates blood pressure through direct vasoconstriction and stimulating aldosterone release, leading to endothelial damage.[58] This damage exacerbates inflammation, enhances oxidative stress, and accelerates plaque formation in arteries. Chronic Ang II exposure further impairs endothelial function and increases the risk of cardiovascular events such as heart attacks and strokes, ultimately contributing to increased mortality.[59] Consistent with previous studies, Ang II initiated HUVECs damage, inhibited NO release, increased ET-1, iNOS and TX-B2 level, and augmented LDH release, further aggravating the course of HTN.[60–62] Furthermore, our cell viability experiment indicated considerable synergy between GAS and GA. Numerous studies have shown that GAS and GA improve the specific mode of action of endothelial cell injury, further supporting our findings.[21,63–66] In our study, synergistic effects are defined as the enhanced efficacy of combining GAS and GA compared to their individual use in attenuating AngII-induced injury. We evaluated this by comparing the outcomes in the combination treatment group with those in the individual treatment groups and the control group. For example, our result show that the combination treatment resulted in a significantly greater increase in cell viability compared to either Gastrodin or Gallic Acid alone.

Pathway enrichment analysis indicated that GAS and GA differentially affected the inflammatory response- and apoptosis-related pathways. The role of the inflammatory response in HTN is significant because it regulates blood pressure by affecting vascular function and endothelial cell activity.[67] Inflammatory factors act on vascular endothelial

and smooth muscle cells, leading to vascular wall inflammation. This, in turn, affects the regulation of vascular tone and blood pressure. For example, TNF-α stimulates the release of NO by vascular endothelial cells, resulting in vasodilation. In contrast, IL-6 increases the sensitivity of vascular endothelial cells to vasoconstrictor factors, leading to vasoconstriction and affecting both the vasodilatory and constrictor functions. Furthermore, apoptosis plays a crucial role in HTN by regulating the structure and function of the vascular wall through its effects on the number and function of vascular endothelial and smooth muscle cells, and by influencing the regulation and maintenance of blood pressure.[68] Abnormal regulation of apoptosis in hypertensive states results in an increased rate of apoptosis in the vascular endothelial and smooth muscle cells. Endothelial cells are a significant component of the vascular lining and their abnormal function is closely linked to vascular wall damage and the development of HTN. Emerging studies suggest that inflammation and apoptosis play crucial roles in the pathogenesis of metabolic dysregulation. Inflammation and apoptosis are intricately linked processes that contribute to metabolic dysregulation through various mechanisms including insulin resistance, adipose tissue dysfunction, and lipid accumulation-induced toxicity.[28,69] Therefore, targeting inflammation and apoptosis pathways holds promise for the development of novel therapeutic strategies to combat metabolic disorders. The current study confirmed that treatment with a combination of GAS (20 μM) and GA (4 μM) markedly increased NO levels, reduced LDH leakage, suppressed the secretion of inflammatory cytokines, decreased the apoptotic cell rate, and alleviated apoptosis-related marker protein levels. Therefore, our results demonstrated that GAS and GA could alleviate Ang II–induced HUVECs injury by inhibiting inflammation and apoptosis. While our study is primarily preclinical, the results suggest that the combination of Gastrodin and Gallic Acid may offer superior therapeutic benefits over their individual use in clinical settings, particularly in the management of chronic inflammation and apoptosis-related diseases. These findings provide a theoretical basis for considering this combination therapy in clinical trials.

Disorders in sphingolipid metabolism affect the occurrence and development of HTN.[15] The development and homeostasis of endothelial cells depend heavily on the proper functioning of sphingolipid metabolism, which is intimately linked to endothelial cell function. Sphingosine, ceramide (Cer), sphingosine 1-phosphate (S1P), serine, sphingosine kinase (SPHK), ceramide kinase (Cerk), and sphingosine 1-phosphate lyase (S1PL) are key sphingolipid metabolites and important enzymes in pathological situations.[14] Numerous inflammatory factors are generated when the downstream inflammation-related signaling pathway is activated, ultimately leading to the destruction of endothelial cell function.[70] In our study, Ang II induced perturbation of sphingolipid metabolism by suppressing the level of S1PR1 and increasing the downstream signaling molecules of ROCK2 and p-NF-κB. In particular, the combination of GAS (20 μM) and GA (4 μM) reversed this phenomenon by elevating the expression of S1PR1 and reducing ROCK2 and p-NF-κB levels. Our study suggests that sphingolipid metabolism is involved in the inhibition of inflammation and apoptosis by GAS and GA in Ang II–induced HUVECs.

Conclusion

In summary, our findings reveals that the combination of GAS and GA significantly mitigates AngII-induced injury in HUVECs by effectively suppressing both inflammation and apoptosis. These effects are closely linked to the modulation of sphingolipid metabolism. Additionally, our findings suggest that targeting sphingolipid metabolism not only provides insights into the progression and severity of HTN but also highlights its potential as a novel therapeutic target for future interventions. This study underscores the promising therapeutic potential of GAS and GA in managing endothelial dysfunction and HTN.

Abbreviations

Ang II, Angiotensin II; HTN, hypertension; TM, Gastrodiae Rhizoma; GQZ, Lycii Fructus; GAS, gastrodin; GA, gallic acid; PHE, 4-hydroxybenzyl alcohol; PA, Parishin A; LBP Lycium barbarum polysaccharides; LUT, luteolin; HUVECs, human umbilical vein endothelial cells; FBS, fetal bovine serum; NO, nitric oxide; LDH, lactate dehydrogenase; IL-6, interleukin-6; IL-1β, interleukin-1β; TNF-α, tumor necrosis factor alpha; OB, oral bioavailability; DL, drug-likeness; PPI, protein-protein interaction; GO, Gene Ontology; KEGG, Kyoto Encyclopedia of Genes and Genomes; BP, biological processes; CC, cellular components; MF, molecular function; CI, combination index; MD, Molecular dynamics simulations; RMSD, Root-mean-square deviation; Rg, Radius of Gyration.

Data Sharing Statement

The data presented in this study are available in the article. For further information or inquiries, please contact the corresponding author.

Ethics Statement

All databases in this study are public databases, the contents of which are publicly available and allow unrestricted reuse through open licenses. The cell lines used in this study do not involve reproductive cloning, chimerism, and heritable genetic manipulation. According to the official document issued by the National Science and Technology Ethics Committee of China, The use of legally obtained public data and the conduct of cellular experiments that do not involve sensitive personal information or commercial interests are not subject to ethical scrutiny (https://www.gov.cn/zhengce/zhengceku/2023-02/28/content_5743658.htm). Therefore, for this study involving public databases and cellular experiments, the need for ethics approval was waived (Ethics Committee of Beijing University of Chinese Medicine). We certify that the study was performed in accordance with the 1964 declaration of HELSINKI and later amendments.

Acknowledgments

The authors extend their gratitude to the researchers and staff involved with the above software and databases.

Author Contributions

All authors made significant contributions to the work reported, whether in the conception, study design, execution, acquisition of data, analysis, and interpretation, or in all these areas, took part in drafting, revising, or critically reviewing the article; gave final approval of the version to be published; agreed on the journal to which the article has been submitted; and agreed to be accountable for all aspects of the work.

Funding

This work was supported by the earmarked fund for China Agriculture Research System (CARS-21), Shaanxi Ningqiang Gastrodia elata Product Development (KJ2022—001).

Disclosure

All authors declare that they have no conflicts of interest regarding this study, and all authors agree to be accountable for all aspects of the work, ensuring integrity and accuracy.

References

1. Mills KT, Stefanescu A, He J. The global epidemiology of hypertension. *Nat Rev Nephrol*. 2020;16(4):223–237. doi:10.1038/s41581-019-0244-2
2. Liberale L, Badimon L, Montecucco F, et al. Inflammation, aging, and cardiovascular disease *JACC* review topic of the week. *J Am Coll Cardiol*. 2022;79(8):837–847. doi:10.1016/j.jacc.2021.12.017
3. Amponsah-Offeh M, Diaba-Nuhoho P, Speier S, Morawietz H. Oxidative stress, antioxidants and hypertension. *Antioxidants*. 2023;12(2):281. doi:10.3390/antiox12020281
4. Calvillo L, Gironacci MM, Crotti L, Meroni PL, Parati G. Neuroimmune crosstalk in the pathophysiology of hypertension. *Nature Reviews Cardiology*. 2019;16(8):476–490. doi:10.1038/s41569-019-0178-1
5. Ma J, Li Y, Yang X, et al. Signaling pathways in vascular function and hypertension: molecular mechanisms and therapeutic interventions. *Signal Trans Targ Ther*. 2023;8(1):168. doi:10.3389/fphar.2023.1113810
6. Treasure CB, Manoukian SV, Klein JL, et al. Epicardial coronary artery responses to acetylcholine are impaired in hypertensive patients. *CircRes*. 1992;71(4):776–781. doi:10.1161/01.Res.71.4.776
7. Xu S, Ilyas I, Little PJ, et al. Endothelial dysfunction in atherosclerotic cardiovascular diseases and beyond: from mechanism to pharmacotherapies. *Pharmacological Rev*. 2021;73(3):924–967. doi:10.1124/pharmrev.120.000096
8. Majolée J, Kovačević I, Hordijk PL. Ubiquitin-based modifications in endothelial cell–cell contact and inflammation. *J Cell Sci*. 2019;132(17): jcs227728. doi:10.1242/jcs.227728
9. Sivasinprasasn S, Pantan R, Thummayot S, Tocharus J, Suksamrarn A, Tocharus CCyanidin-3-glucoside attenuates angiotensin II-induced oxidative stress and inflammation in vascular endothelial cells. *Chemico-Biological Interact*. 2016;28(S0009–27970016):30510–30515. doi:10.1016/j.cbi.2016.10.022
10. Paz Ocaranza M, Riquelme JA, García L, et al. Counter-regulatory renin-angiotensin system in cardiovascular disease. *Nat Rev Cardiology*. 2020;17(2):116–129. doi:10.1038/s41569-019-0244-8
11. Cheng ZJ, Vapaatalo H, Mervaala E. Angiotensin II and vascular inflammation. *Med Sci Monitor*. 2005;11(6):RA194–RA205.

12. Eckardt K-U. Oxygen sensing and cell metabolism in inflammation. *Nat Rev Nephrol*. 2017;13(12):727–728. doi:10.1038/nrneph.2017.145
13. Lee M, Lee SY, Bae Y-S. Functional roles of sphingolipids in immunity and their implication in disease. *Expe Molecular Med*. 2023;55 (6):1110–1130. doi:10.1038/s12276-023-01018-9
14. Lai YL, Tian Y, You XT, Du JN, Huang JM. Effects of sphingolipid metabolism disorders on endothelial cells. *Lipids Health Dis*. 2022;21(1):12. doi:10.1186/s12944-022-01701-2
15. Cantalupo A, Zhang Y, Kothiya M, et al. Nogo-B regulates endothelial sphingolipid homeostasis to control vascular function and blood pressure. *Nature Med*. 2015;21(9):1028–1037. doi:10.1038/nm.3934
16. Zhu C, Zhang Z, Wang S, Sun Z. Study on the mechanism of gastrodiae rhizoma, lycii fructus, and ziziphi spinosae semen in sedation and tranquillising mind. *Mol Divers*. 2023;45(3):1–16. doi:10.1007/s11030-023-10756-x
17. Ahn E-K, Jeon H-J, Lim E-J, Jung H-J, Park E-H. Anti-inflammatory and anti-angiogenic activities of *Gastrodia elata* Blume. *J Ethnopharmacology*. 2007;110(3):476–482. doi:10.1016/j.jep.2006.10.006
18. Jiang Y-H, Zhang P, Tao Y, et al. Banxia baizhu tianma decoction attenuates obesity-related hypertension. *J Ethnopharmacology*. 2021;266 (11):34–53. doi:10.1016/j.jep.2020.113453
19. Ma R-H, Zhang -X-X, Ni Z-J, et al. *Lycium barbarum* (Goji) as functional food: a review of its nutrition, phytochemical structure, biological features, and food industry prospects. *Crit Rev Food Sci Nutr*. 2023;63(30):10621–10635. doi:10.1080/10408398.2022.2078788
20. de Oliveira LM, de Oliveira TS, da Costa RM, et al. The vasorelaxant effect of gallic acid involves endothelium-dependent and -independent mechanisms. *Vasc Pharmacol*. 2016;81(6):9–74. doi:10.1016/j.vph.2015.10.010
21. Kang N, Lee J-H, Lee W, et al. Gallic acid isolated from *Spirogyra* sp. improves cardiovascular disease through a vasorelaxant and antihypertensive effect. *Environ Toxicol Pharmacol*. 2015;39(2):764–772. doi:10.1016/j.etap.2015.02.006
22. Cao Y, Gong Y, Liu L, et al. The use of human umbilical vein endothelial cells (HUVECs) as an *in vitro* model to assess the toxicity of nanoparticles to endothelium: a review. *J Appl Toxicol*. 2017;37(12):1359–1369. doi:10.1002/jat.3470
23. Duranova H, Kuzelova L, Borotova P, Simora V, Fialkova V. Human umbilical vein endothelial cells as a versatile cellular model system in diverse experimental paradigms: an ultrastructural perspective. *Microsc microanal*. 2024;30(3):419–439. doi:10.1093/mam/ozae048
24. Wolf G, Wenzel UO. Angiotensin II and cell cycle regulation. *Hypertension*. 2004;43(4):693–698. doi:10.1161/01.HYP.0000120963.09029.ca
25. Re RN. Role of intracellular angiotensin II. *Am J Physiol-Heart Circul Physiol*. 2018;314(4):H766–H771. doi:10.1152/ajpheart.00632.2017
26. Guo Z, Yang X, Wu M, et al. Gastrodin attenuates angiotensin II-induced vascular contraction and MLCK/p-MLC $_2$ pathway activation. *Pharm Biol*. 2023;61(1):858–867. doi:10.1080/13880209.2023.2207591
27. Xiao GR, Tang R, Yang N, Chen YH. Review on pharmacological effects of gastrodin. *Arch Pharm Res*. 2023;46(9–10):744–770. doi:10.1007/s12272-023-01463-0
28. Potterat O. Goji (*Lycium barbarum* and *L-chinense*): phytochemistry, pharmacology and safety in the perspective of traditional uses and recent popularity. *Planta Med*. 2010;76(1):7–19. doi:10.1055/s-0029-1186218
29. Zhou BJ, Xia H, Yang LG, Wang SK, Sun GJ. The effect of Lycium barbarum polysaccharide on the glucose and lipid metabolism: a systematic review and meta-analysis. *J Am Nutrition Assoc*. 2022;41(6):618–626. doi:10.1080/07315724.2021.1925996
30. Baudin B, Bruneel A, Bosselut N, Vaubourdolle M. A protocol for isolation and culture of human umbilical vein endothelial cells. *Nat Protoc*. 2007;2(3):481–485. doi:10.1038/nprot.2007.54
31. Yang LL, Li D-Y, Zhang Y-B, et al. Salvianolic acid A inhibits angiotensin II-induced proliferation of human umbilical vein endothelial cells by attenuating the production of ROS. *Acta Pharmacol Sin*. 2012;33(1):41–48. doi:10.1038/aps.2011.133
32. Chou TC. Drug combination studies and their synergy quantification using the chou-talalay method. *Cancer Res*. 2010;70(2):440–446. doi:10.1158/0008-5472.Can-09-1947
33. Li X, Hou R, Qin X, et al. Synergistic neuroprotective effect of saikosaponin A and albiflorin on corticosterone-induced apoptosis in PC12 cells via regulation of metabolic disorders and neuroinflammation. *Mol Biol Rep*. 2022;49(9):8801–8813. doi:10.1007/s11033-022-07730-5
34. Dang HM, Song BR, Dong R, Zhang HJ. Atorvastatin reverses the dysfunction of human umbilical vein endothelial cells induced by angiotensin II. *Exp Ther Med*. 2018;16(6):5286–5297. doi:10.3892/etm.2018.6846
35. Guo CL, Liu HM, Li B, Lu ZY. Angiotensin-(1-9) prevents angiotensin II-induced endothelial apoptosis through CNPY2/PERK pathway. *Apoptosis*. 2023;28(3–4):379–396. doi:10.1007/s10495-022-01793-2
36. Livak KJ, Schmittgen TD. Analysis of relative gene expression data using real-time quantitative PCR and the 2− ΔΔCT method. *methods*. 2001;25 (4):402–408. doi:10.1006/meth.2001.1262
37. Lin WT, Jiang Y-C, Mei Y-L, et al. Endothelial deubiquinatase YOD1 mediates Ang II-induced vascular endothelial-mesenchymal transition and remodeling by regulating β-catenin. *Acta Pharmacol Sin*. 2024;45(8):1618–1631. doi:10.1038/s41401-024-01278-9
38. Pronk S, Páll S, Schulz R, et al. GROMACS 4.5: a high-throughput and highly parallel open source molecular simulation toolkit. *Bioinformatics*. 2013;29(7):845–854. doi:10.1093/bioinformatics/btt055
39. Zhong Y, Zhao YF, Meng X, Wang F, Zhou L. Unveiling the mechanism of Liangxue Siwu decoction in treating rosacea through network pharmacology and in-vitro experimental validation. *J Inflamm Res*. 2024;17(1):5685–5699. doi:10.2147/jir.S471097
40. Pantsar T, Poso A. Binding affinity via docking: fact and fiction. *Molecules*. 2018;23(8):11. doi:10.3390/molecules23081899
41. STd M, Giatti L, Brant LCC, et al. Hypertension, prehypertension, and hypertension control. *Hypertension*. 2021;77(2):672–681. doi:10.1161/HYPERTENSIONAHA.120.16080
42. Zhang D-Y, Cheng Y-B, Guo Q-H, et al. Treatment of masked hypertension with a Chinese herbal formula: a randomized, placebo-controlled trial. *Circulation*. 2020;142(19):1821–1830. doi:10.1161/CIRCULATIONAHA.120.046685
43. Zhang Q, et al. Cocktail of astragalus membranaceus and radix trichosanthis suppresses melanoma tumor growth and cell migration through regulation of Akt-related signaling pathway. *Front Pharmacol*. 2022;13(88):2–15. doi:10.3389/fphar.2022.880215
44. Li J, Zhang X, Guo D et al. The mechanism of action of paeoniae radix rubra–angelicae sinensis radix drug pair in the treatment of rheumatoid arthritis through PI3K/AKT/NF-κB signaling pathway. *Front Pharmacol*. 2023;14(11):138–150. doi:10.3389/fphar.2023.1113810
45. Sun XN, Jia B, Sun J, et al. Gastrodia elata Blume: a review of its mechanisms and functions on cardiovascular systems. *Fitoterapia*. 2023;167 (1):5–11. doi:10.1016/j.fitote.2023.105511
46. Zhang XY, Yang X, Lin Y, et al. Anti-hypertensive effect of *Lycium barbarum* L. with down-regulated expression of renal endothelial lncRNA sONE in a rat model of salt-sensitive hypertension. *Int J Clin Exp Pathol*. 2015;8(6):6981–6987.

47. Zhu HD, Yao Y, Luo Z, et al. Gastrodia elata blume polysaccharides: a review of their acquisition, analysis, modification, and pharmacological activities. *Molecules*. 2019;24(13):18. doi:10.3390/molecules24132436
48. Gong MQ, Lai -F-F, Chen J-Z, et al. Traditional uses, phytochemistry, pharmacology, applications, and quality control of gastrodia elata blume: a comprehensive review. *J Ethnopharmacology*. 2024;319(Pt 1):117128. doi:10.1016/j.jep.2023.117128
49. Yan X, Zhang Q-Y, Zhang Y-L, et al. Gallic acid attenuates angiotensin II-induced hypertension and vascular dysfunction by inhibiting the degradation of endothelial nitric oxide synthase. *Front Pharmacol*. 2020;11(1):1–21. doi:10.3389/fphar.2020.01121
50. Jin L, Lin MQ, Piao ZH, et al. Gallic acid attenuates hypertension, cardiac remodeling, and fibrosis in mice with N^G-nitro-L-argininemethyl ester-induced hypertension via regulation of histone deacetylase 1or histone deacetylase 2. *J Hypertens*. 2017;35(7):1502–1512. doi:10.1097/hjh.0000000000001327
51. Dai B, Liu CF, Zhang S, Huang M, Yin SG. Gastrodin suppresses the progression of atherosclerosis and vascular inflammation by regulating TLR4/NF-κB pathway. *Cell Biochem Biophys*. 2024;82(2):697–703. doi:10.1007/s12013-024-01218-8
52. Bai JR, Zhang Y, Tang C, et al. Gallic acid: pharmacological activities and molecular mechanisms involved in inflammation-related diseases. *Biomed Pharmacother*. 2021;133(1):4–15. doi:10.1016/j.biopha.2020.110985
53. Shiu PHT, et al. Anti-inflammatory effect of gallic acid on HaCaT keratinocytes through the inhibition of MAPK-, NF-kB-, and Akt-dependent signaling pathways. *Bangladesh J Pharmacol*. 2023;18(1):24–32. doi:10.3329/bjp.v18i1.62914
54. Chu C, Chu C, Ru H, Chen Y, Xu J, Wang C, Jin YGallic acid attenuates LPS-induced inflammation in Caco-2 cells by suppressing the activation of the NF-κB/MAPK signaling pathway. *Acta Biochim Biophys Sin*. 2024;56(6):905–915. doi:10.3724/abbs.2024008
55. Al Zahrani NA, El-Shishtawy RM, Asiri AM. Recent developments of gallic acid derivatives and their hybrids in medicinal chemistry: a review. *Eur J Med Chem*. 2020;204(3):73–89. doi:10.1016/j.ejmech.2020.112609
56. Xue XF, Li F, Xu M, et al. Gastrodin ameliorates atherosclerosis by inhibiting foam cells formation and inflammation through down-regulating NF-κB pathway. *Nutr Metab*. 2023;20(1):10. doi:10.1186/s12986-022-00722-z
57. Verma K, Pant M, Paliwal S, Dwivedi J, Sharma S. An insight on multicentric signaling of angiotensin ii in cardiovascular system: a recent update. *Front Pharmacol*. 2021;12(7):1–15. doi:10.3389/fphar.2021.734917
58. Kaparianos A, Argyropoulou E. Local renin-angiotensin II systems, angiotensin-converting enzyme and its homologue ACE2: their potential role in the pathogenesis of chronic obstructive pulmonary diseases, pulmonary hypertension and acute respiratory distress syndrome. *Curr Med Chem*. 2011;18(23):3506–3515. doi:10.2174/092986711796642562
59. Ferrario CM. Role of angiotensin II in cardiovascular disease - Therapeutic implications of more than a century of research. *J. Renin-Angiotensin-Aldosterone Syst*. 2006;7(1):3–14. doi:10.3317/jraas.2006.003
60. Ji C, Yu Y, Zhang M, Yu W, Dong S. Loxoprofen sodium alleviates oxidative stress and apoptosis induced by angiotensin II in human umbilical vein endothelial cells (HUVECs). *Drug Design, Develop Ther*. 2020;14:5087–5096. doi:10.2147/DDDT.S266175
61. Cai S, Pan N, Xu M, et al. ACE inhibitory peptide from skin collagen hydrolysate of Takifugu bimaculatus as potential for protecting HUVECs injury. *Marine Drugs*. 2021;19(12):655. doi:10.3390/md19120655
62. Dimmeler S, Rippmann V, Weiland U, Haendeler J, Zeiher AM. Angiotensin II induces apoptosis of human endothelial cells: protective effect of nitric oxide. *CircRes*. 1997;81(6):970–976. doi:10.1161/01.res.81.6.970
63. Lin JL, Shi Y, Miao J, et al. Gastrodin alleviates oxidative stress-induced apoptosis and cellular dysfunction in human umbilical vein endothelial cells via the nuclear factor-erythroid 2-related factor 2heme oxygenase-1 pathway and accelerates wound healing in vivo. *Front Pharmacol*. 2019;10:1273. doi:10.3389/fphar.2019.01273
64. Chen JY, Huang YL, Hu XC, Bian XH, Nian SH. Gastrodin prevents homocysteine-induced human umbilical vein endothelial cells injury via PI3K/Akt/eNOS and Nrf2/ARE pathway. *J Cell Mol Med*. 2021;25(1):345–357. doi:10.1111/jcmm.16073
65. Ma L, Zhu X-F, Wu -Y-Y, et al. Protective effect of propyl gallate against oxidized low-density lipoprotein-induced injury of endothelial cells. *Chin J Integrative Med*. 2015;21(4):299–306. doi:10.1007/s11655-014-1980-6
66. Buachan P, Chularojmontri L, Wattanapitayakul SK. Selected activities of citrus maxima merr. fruits on human endothelial cells: enhancing cell migration and delaying cellular aging. *Nutrients*. 2014;6(4):1618–1634. doi:10.3390/nu6041618
67. Zhang ZL, Zhao L, Zhou XY, Meng X, Zhou XL. Role of inflammation, immunity, and oxidative stress in hypertension: new insights and potential therapeutic targets. *Front Immunol*. 2023;13:1098725. doi:10.3389/fimmu.2022.1098725
68. Jurasz P, Courtman D, Babaie S, Stewart DJ. Role of apoptosis in pulmonary hypertension: from experimental models to clinical trials. *Pharmacol Ther*. 2010;126(1):1–8. doi:10.1016/j.pharmthera.2009.12.006
69. Hotamisligil GS. Inflammation, metaflammation and immunometabolic disorders. *Nature*. 2017;542(7640):177–185. doi:10.1038/nature21363
70. Borodzicz-Jazdzyk S, Jazdzyk P, Lysik W, Cudnoch-Jedrzejewska A, Czarzasta K. Sphingolipid metabolism and signaling in cardiovascular diseases. *Front Cardiovasc Med*. 2022;9:915961. doi:10.3389/fcvm.2022.915961